

Accepted Manuscript

DMXAA-pyranoxanthone hybrids enhance inhibition activities against human cancer cells with multi-target functions

Jie Liu, Fan Zhou, Lei Zhang, Huailing Wang, Jianrun Zhang, Cao Zhang, Zhenlei Jiang, Yanbing Li, Zhijun Liu, Heru Chen



PII: S0223-5234(17)30876-0

DOI: [10.1016/j.ejmech.2017.10.074](https://doi.org/10.1016/j.ejmech.2017.10.074)

Reference: EJMECH 9866

To appear in: *European Journal of Medicinal Chemistry*

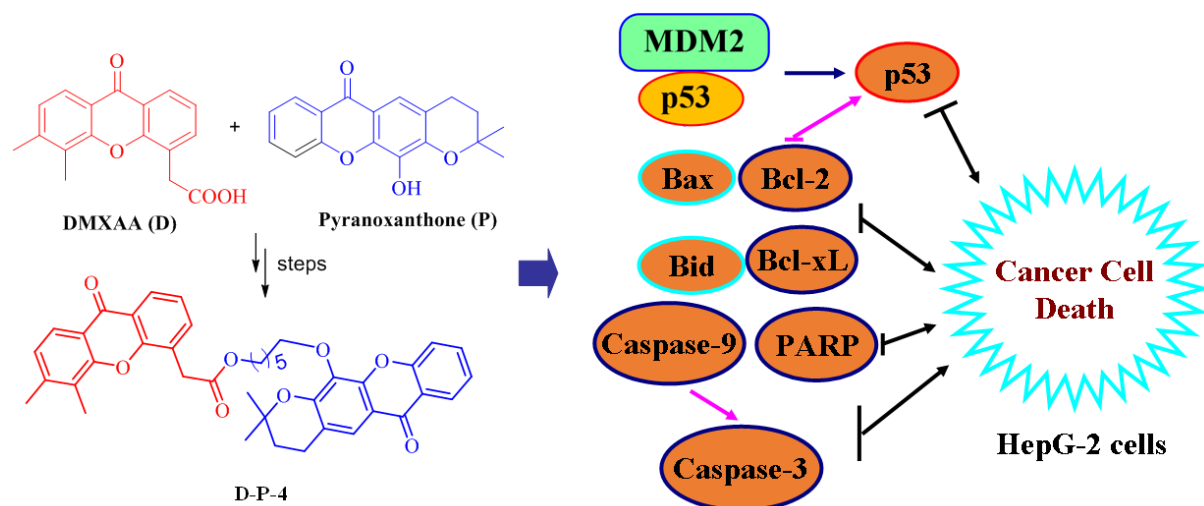
Received Date: 4 July 2017

Revised Date: 25 October 2017

Accepted Date: 27 October 2017

Please cite this article as: J. Liu, F. Zhou, L. Zhang, H. Wang, J. Zhang, C. Zhang, Z. Jiang, Y. Li, Z. Liu, H. Chen, DMXAA-pyranoxanthone hybrids enhance inhibition activities against human cancer cells with multi-target functions, *European Journal of Medicinal Chemistry* (2017), doi: 10.1016/j.ejmech.2017.10.074.

This is a PDF file of an unedited manuscript that has been accepted for publication. As a service to our customers we are providing this early version of the manuscript. The manuscript will undergo copyediting, typesetting, and review of the resulting proof before it is published in its final form. Please note that during the production process errors may be discovered which could affect the content, and all legal disclaimers that apply to the journal pertain.



**DMXAA-Pyranoxanthone hybrids enhance inhibition activities
against human cancer cells with multi-target functions**

Jie Liu^a, Fan Zhou^a, Lei Zhang^a, Huailing Wang^b, Jianrun Zhang^a, Cao Zhang^a,
Zhenlei Jiang^a, Yanbing Li^a, Zhijun Liu^a, Heru Chen^{*a, c}

^a *Institute of Traditional Chinese Medicine and Natural Products, College of Pharmacy, Jinan University, Guangzhou 510632, P. R. China*

^b *School of Food Sciences and Engineering, South China University of Technology, Guangzhou 510641, China*

^c *Guangdong Province Key Laboratory of Pharmacodynamic Constituents of TCM and New Drugs Research, Jinan University, Guangzhou 510632, P. R. China*

** Corresponding authors:*

Prof. Dr. Heru Chen

Huangpu Avenue West 601

Institute of Traditional Chinese Medicine and Natural Product

College of Pharmacy, Jinan University

Guangzhou 510632, P. R. China

Tel: +86-20-38375299; Fax: +86-20-85221559

E-mail: thrchen@jnu.edu.cn

Abstract Four 5,6-dimethylxanthone-4-acetic acid (**D**) and pyranoxanthone (**P**) hybrids (**D-P-n**) were design-synthesized based on multi-target-addressed strategy. **D-P-4** was confirmed as the most active agent against HepG-2 cell line growth with an IC_{50} of $0.216 \pm 0.031 \mu M$. Apoptosis analysis indicated different contributions of early/late apoptosis/necrosis to cell death for both monomers, the combination (**D+P** in 1:1 mol ratio) and **D-P-4**. They all arrested more cells on S phase. Western Blot implied that **D-P-4** regulated p53/MDM2 to a better healthy state. Moreover, it improved Bax/Bcl-2 signaling pathway to increase cancer cell apoptosis. In all cases studied, **D-P-4** showed the best activity and synergistic effect. All the evidences support that **D-P-4** is a better anti-cancer therapy with multi-target functions.

Keywords: xanthones; anti-cancer; multi-targets-addressed ligand; synergistic effect; p53/MDM2; Bax/Bcl-2

1. Introduction

The multi-target approach has been suggested as particularly suitable to struggle the heterogeneity and the multifactorial nature of cancer [1]. This strategy involves the concept of a single chemical entity with desirable activity at more than one biological target. The designed multiple ligands (DMLs), which may also be described as multiple-target directed ligands, heterodimers, promiscuous drugs and pan-agonists, are drugs which act at multiple biomolecular targets. No doubt, the successful treatment of these ligands often depends on pharmaceutical intervention at multiple pathways, with a combination of different drugs in one single entity [2-5].

Many DMLs have been successfully applied to improve the anticancer efficacy. For example, CS2164 (**Fig. 1**), named as (*N*-(2-aminophenyl)-6-6-[(7-methoxy-4-quinolinyl)oxy]-1-naphthalene-carboxamide, was designed and evaluated as a novel orally active multi-target inhibitor that simultaneously inhibits the angiogenesis-related kinases (VEGFR2, VEGFR1, VEGFR3, PDGFR α and c-Kit), mitosis-related kinase Aurora B and chronic inflammation-related kinase CSF-1R in a high potency manner with the IC₅₀ value at a single-digit nanomolar range [6]. Yan, et al. designed and synthesised a series of benzoselenazole-stilbene hybrids by combining the pharmacophores of resveratrol and ebselen, and showed that compound **6e** (**Fig. 1**) had the optimal activity against four human cell lines. It induces G2/M cell cycle arrest and apoptosis of the human liver carcinoma Bel-7402 cell line and exhibits the best thioredoxin reductase (TrxR) inhibitory activity amongst all the tested compounds [7]. The oxime analog **7e** (**Fig. 1**) was indicated as inhibitors of tubulin polymerization, BRAFV^{600E}, FAK and EGFR-TK; and it also exhibited multiple drug resistant (MDR) reversal activity [4].

Intriguing by the interesting scaffolds and pharmacological importance of xanthenes (**Fig. 1**), our group have been pursuing the search for novel xanthenes by either isolation from nature or synthesis design [8-10]. It is of notice that many xanthone compounds are reported with anticancer activity [11]. Among them, two xanthenes, 5,6-dimethylxanthone-4-acetic acid (DMXAA) and 3,4-dihydro-12-

hydroxy-2,2-dimethyl-2*H*,6*H*-pyrano[3,2-*b*]xanthen-6-one (pyranoxanthone) (**Fig. 1**) [12,13] caught our eyes. As reported, DMXAA is the first small-molecule vascular-disrupting agent to enter phase III clinical trial stage [14]; and pyranoxanthone is a novel small-molecule inhibitor of p53-MDM2 interaction with a xanthone scaffold, in which p53 is a tumor suppressor and MDM2 (murine double minute 2) is the main endogenous negative regulator against p53.

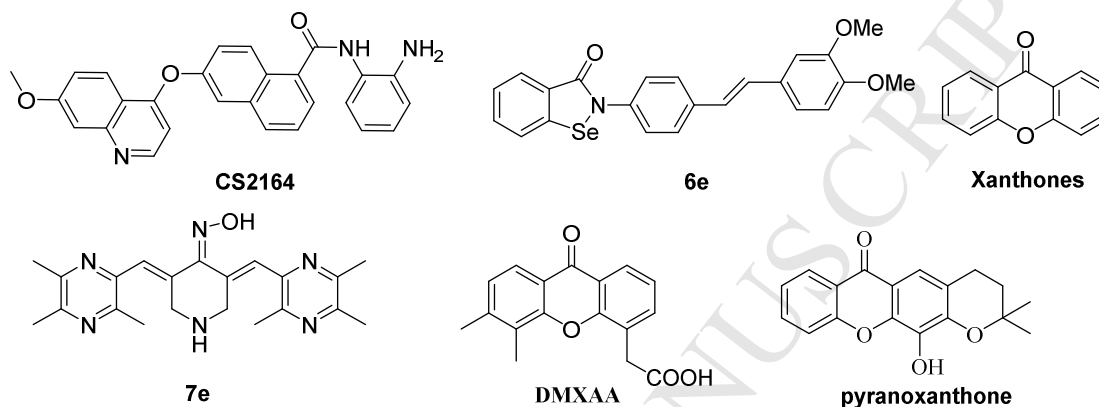


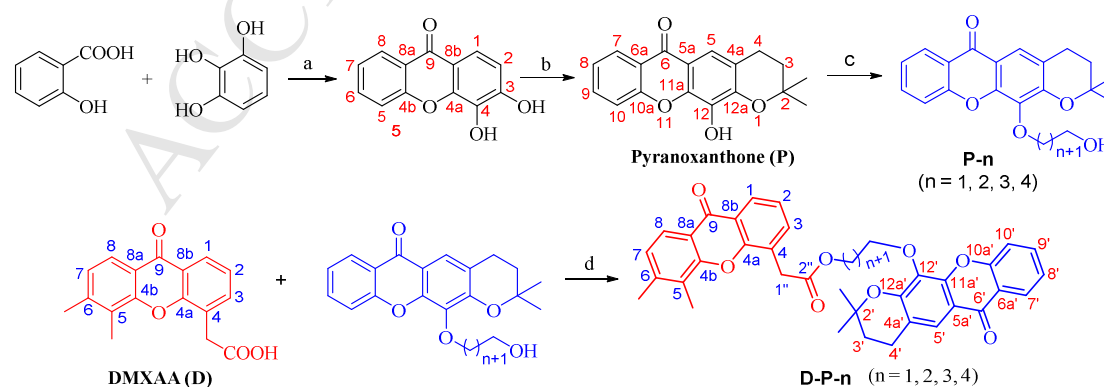
Fig. 1. Chemical structures of some DMLs and xanthenes.

However, DMXAA is not a particularly potent drug, with dose levels of up to 4.9 g/m² reported in human trial [15]. Moreover, the side effects of paropsia, uracratia and dysphoria limit its use in clinic [16]. How to improve the anti-cancer efficacy of DMXAA is what we are concerning about. Recently, we disclosed that DMXAA can regulate p53/MDM2 to a better healthy state, although the activity is weaker than that of its combination [10]. Therefore, it is reasonable for us to suggest that pyranoxanthone, which also has the same ability to adjust p53/MDM2 interaction, may probably synergize with DMXAA to improve the anticancer efficacy by DML design or in the form of combination.

Hence, here in the current study, a series of DMXAA (**D**) and pyranoxanthone (**P**) hybrids were design-synthesized. The screening of the inhibition activity against human cancer cell lines of these hybrids and the D/P combination were carried on. Furthermore, the mechanism of how the candidate hybrid induces the death of HepG-2 liver cancer cells will be also disclosed thereafter.

2. Chemistry

As outlined in **Scheme 1**, the syntheses of DMXAA/pyranoxanthone hybrids (**D-P-n**, $n = 1, 2, 3, 4$) firstly began with the syntheses of DMXAA and pyranoxanthone. DMXAA was prepared based in a process early described [17]. While pyranoxanthone was made using salicylic acid and pyrogallol as starting materials. In step a, condensation of salicylic acid with 1,2,3-trihydroxybenzene to 3,4-dihydroxyxanthone was successfully carried on by applying a modified method early described [10], in which anhydrous zinc chloride (ZnCl_2) and phosphorus oxychloride (POCl_3) was used as both catalyst and solvent under the assistance of microwave radiation. The yield was 79.5%. The construction of 2,2-dimethyl-2*H*,6*H*-pyrano[3,2-*b*] moiety was completed using montmorillonite K10 as catalyst assisted by microwave radiation, leading to pyranoxanthone with a yield of 38.5%. 4-Hydroxyalkylation of pyranoxanthone was realized under a mild conditions, in which potassium carbonate (K_2CO_3) was applied as a base, resulted in a series of 4-hydroxyalkyl pyranoxanthone (**P-n**, $n = 1, 2, 3, 4$). Yields lied between 80-90%. DMXAA condensated with **P-n** applied dicyclohexyldiimide (DCC) as coupling reagent to offer **D-P-n** hybrids in a yield of 48%-53%. The coupling reactions were benefited from the addition of 4-*N,N*-dimethylaminopyridine (DMAP). All the four hybrids were characterized by NMR and MS. And their purities were analyzed by RP-HPLC method.



Scheme 1. Syntheses of DMXAA/pyranoxanthone hybrids. Conditions and Agents: (a) $\text{ZnCl}_2/\text{POCl}_3$, microwave (MW), 40 min; (b) $\text{BrCH}_2\text{CH}(\text{CH}_3)_2$, MW/600 W, montmorillonite

K10 (20 equiv.), CHCl_3 , 40 min; (c) $\text{Br}(\text{CH}_2)_m\text{OH}$ ($m = 3, 4, 5, 6$) (dropwise, 30 min), K_2CO_3 , DMF, r. t., 24 h; (d) DCC/DMAP.

3. Results and discussion

3.1. Growth inhibitory effects of D-P hybrids and the combination against human cancer cell lines

It's the common sense that breast cancer, liver cancer, chronic myelogenous leukemia, and colorectal adenocarcinoma are very popular cancer types, this is the reason why Michigan Cancer Foundation-7 (MCF-7), human breast MDA-MB-231, human liver Hep-G2, and chronic myelogenous leukemia K562 cancer cell lines were chosen as materials in the current study. MTT assay, in which 3-(4,5-dimethylthiazol-2-yl)-2,5-diphenyl tetrazolium bromide was used as a dye, was applied to determine the effects of **D/P** hybrids and **D/P** combination on the cellular growth inhibition. As shown in **Table 1**, compared with DMXAA and Pyranoxanthone monomer, **D/P** combination, which is the mixture of 1:1 molar ration of **D** and **P**, was showed greater anti-proliferation activity against all the tested cancer cell lines. However, more excitingly, the **D-P-4** hybrid exhibited significant inhibitory activity enhancement against all the tested cancer cell lines, particularly MCF-7 and HepG-2. Compared with DMXAA, the inhibition activity of **D-P-4** against MCF-7 was increased by 100 times with IC_{50} value of $0.534 \pm 0.043 \mu\text{M}$; and against HepG-2 by 460 times with IC_{50} value of $0.216 \pm 0.031 \mu\text{M}$.

Generally speaking, all the hybrids were confirmed with enhancing effect depending on the chain length of the spacer. The longer the carbon chain, the better the inhibition activity. When the carbon is more than 5 (**D-P-3** and **D-P-4**), the inhibition activity of the hybrid against all the tested cancer cell lines is better that that of **D/P** combination (in 1:1 molar ratio). This synergistic effect might be ascribed to the conformation changes brought about by the spacer. When the spacer is a short carbon chain (< 5), the hybrid is in a more compacted conformation and can only fit into one pocket of the target protein; However, when the spacer is a long carbon chain (> 5), the hybrid is in a flexible, stretched conformation, and may probably bind to

more than one pocket of the target protein, or bind to two targets. Whether the six carbon chain spacer is the optimal needs further investigations.

Table 1. Cell growth inhibition of synthesized **D/P** hybrids and combination

Compound	IC ₅₀ ^a (μM)			
	MDA-MB-231	MCF-7	HepG2	K562
DMXAA (D) ^b	48.44 ± 7.41	54.41 ± 6.43	100.2 ± 11.24	57.44 ± 6.15
Pyranoxanthone (P)	59.32 ± 6.82	101.5 ± 11.72	40.31 ± 5.12	27.82 ± 3.20
P-4	97.31 ± 9.97	138.7 ± 15.85	99.07 ± 10.08	109.51 ± 11.41
D+P (1 : 1)	12.12 ± 1.63	11.89 ± 1.23	21.25 ± 2.73	19.14 ± 2.53
D-P-1	32.21 ± 3.31	51.74 ± 6.74	32.72 ± 3.42	32.31 ± 4.11
D-P-2	19.63 ± 2.14	33.22 ± 3.72	11.92 ± 1.52	20.63 ± 2.27
D-P-3	11.24 ± 1.37	8.723 ± 1.10	1.529 ± 0.23	15.03 ± 1.84
D-P-4	1.129 ± 0.13	0.534 ± 0.043	0.216 ± 0.031	9.13 ± 1.34

^a IC₅₀ values are shown as mean ± standard error of the mean (SD), from at least three independent experiments.

^b DMXAA was used as a positive control.

Since the existence of ester bond in **D-P-n**, they are expected to be hydrolyzed easily by enzyme *in vivo*. Therefore, investigation on the stability of the hybrid was a must. As the most active compound, the stability of **D-P-4** in cell culture medium and mouse serum was studied. It was found that the half life time ($t_{1/2}$) of **D-P-4** in cell culture medium and mouse serum was 24.8 h, and 4.2 h, respectively (**Fig. 2**). Obviously, **D-P-4** has a certain degree of stability in either cell culture medium or mouse serum. It is more stable in cell culture medium than that in mouse serum.

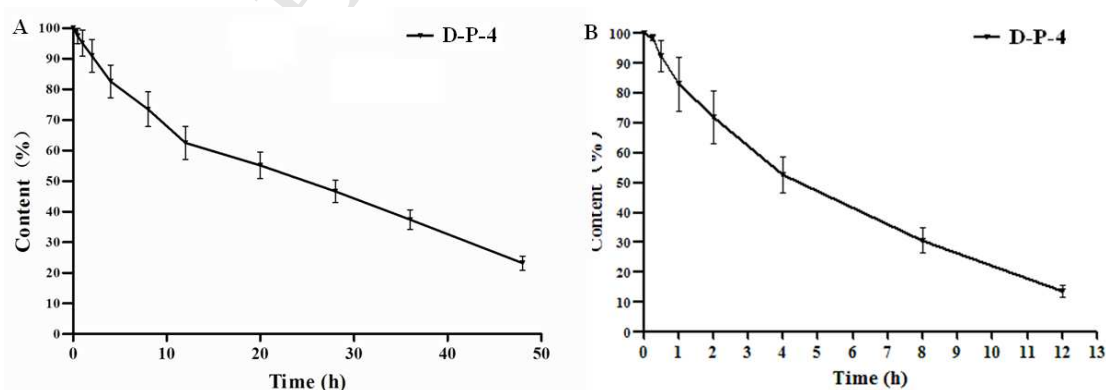


Fig. 2. Stability of **D-P-4** in (A) in cell culture medium; and (B) mouse serum. 1 ml solution of 10 μM/L **D-P-4** was suspended with 4 ml of mouse serum, and then incubated at 37°C. 10 μl of the mixed solution was taken at the time point of (A) 0, 0.25, 0.5, 1, 2, 4, 8, 12, 20, 28, 36, 48 h, respectively; or (B) 0, 0.5, 1, 2, 4, 8, 12 h, respectively. These samples were pretreated with

methanol and 20% perchloric acid, centrifuged at 10000 r/min for 5 minutes. Then the supernatant was submitted to HPLC for content analysis. Each experiments was repeated 4 times.

After hydolysis of **D-P-4**, the resulted products are **DMXAA** and **P-4**. The inhibition activity of **P-4** against four cancer cell lines was also determined. It was shown that the introduction of 6-hydroxyhexyl group at 12-*O* position caused the decreased of inhibition activity. This may exclude the possibility that the activity enhancement of **D-P-4** is depended on the release of **P-4**.

The current evidence support that the **D-P-4** is probably a promising anticancer therapy. Therefore, the cytotoxicity against normal cell line from healthy tissues must be evaluated. Here, the inhibition against the growth of normal cell line was determined. The testing method is the same as that applied to cancer cell line. It was found that the cytotoxicities of **DMXAA** against human liver cell line HL-7702 and mouse embryo fibroblast cell line NIH/3T3 are almost at the same level compared to that against cancer cell lines, in which the IC_{50} values are $101.3 \pm 2.6 \mu\text{M}$ to HL-7702, and $67.8 \pm 1.3 \mu\text{M}$ to NIH/3T3. However, the cytotoxicities of **D-P-4** against normal cells are far less than that against cancer cell lines. The IC_{50} value is $452.29 \pm 41.20 \mu\text{M}$ (for 24 h), and $351.98 \pm 31.26 \mu\text{M}$ (for 48 h) against HL-7702 cell line, respectively; while the IC_{50} value is $378.03 \pm 37.22 \mu\text{M}$ (for 24 h), and $293.22 \pm 25.34 \mu\text{M}$ (for 48 h) against HL-7702 cell line, respectively. Compared the IC_{50} values at the same incubation time (24 h), the cytotoxicity against HL-7702 cells is 2092 times less than that against HepG-2 cancer cells. Definitely, **D-P-4** significantly showed attenuated cytotoxicity effect against normal cells.

3.2. Cell death induced by pyranoxanthone, **DMXAA**, **D/P** combination and **D-P-4**

Since **D-P-4** was indicated with the greatest enhancing effect against HepG-2 (**Table 1**), together with the fact that Hepatocellular carcinoma (HCC) is one of the most common malignancies around the world, accounting for over 80% of all liver cancers with extremely poor prognosis [18], the development for of novel and effective therapies for this devastating disease is urgently needed. This is the reason

why we chose HepG-2 cell line to explore the mechanisms involved in how these agents prevent the cancer cell growth.

Flow cytometry using propidium iodide (PI) and Annexin-V as dyes to label viable and dead cells is one of the common technique to study cell apoptosis/necrosis, therefore it was applied here. As shown in **Fig. 3**, at the same dose of 0.2 μ M, pyranoxanthone caused less than 10% total apoptosis/necrosis rate; While DMXAA (**D**) showed better inhibition activity than pyranoxanthone (**P**), in which about 20% total apoptosis/necrosis rate (with 13% for early and 7% for late) was found. Interestingly, the combination (**D+P** in 1:1 mol ratio) was found inducing 61% total apoptosis/necrosis rate (with 15% for early and 46% for late). More excitingly, **D-P-4** hybrid was indicated with the greatest inhibition activity, in which it led to 80% total apoptosis/necrosis rate (with 38% for early and 42% for late). It was shown that **D-P-4** induced almost the same late apoptosis/necrosis rate but greater early apoptosis/ necrosis rate than the combination (**D+P**).

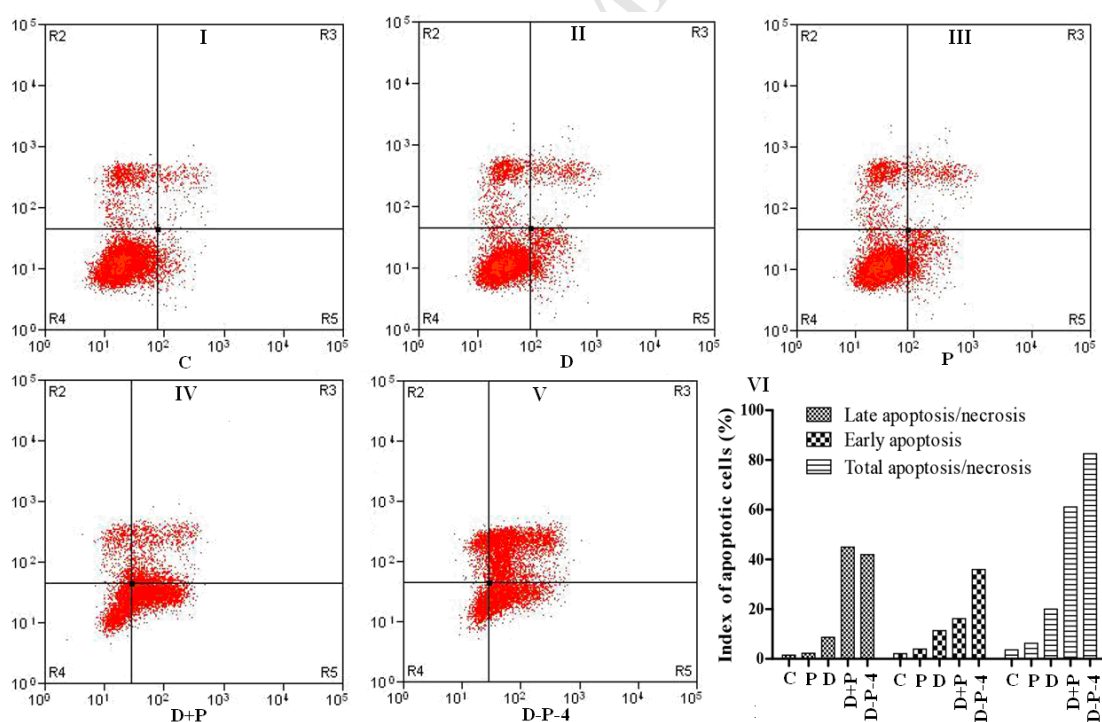


Fig. 3. DMXAA (**D**), pyranoxanthone (**P**), the combination (**D+P**) and **D-P-4** induced apoptosis in HepG-2 cells. Representative scatter diagrams. HepG-2 cells were pre-treated without the addition of any samples, the control (**C**) (**I**); with a dose of 0.2 μ M **D** (**II**), **P** (**III**), **D+P** (1:1 mol ratio) (**IV**), and **D-P-4** (**V**), respectively for 24 h. Cells were stained with Annexin-V and PI. The apoptosis of HepG-2 cells was detected by flow cytometry. The evaluation of apoptosis is via Annexin V: FITC

Apoptosis Detection Kit per manufacture's protocol. The quantitative results were shown in (VI). In each scatter diagrams, the abscissa represents the fluorescence intensity of the cells dyed by Annexin V; and the ordinate represents the fluorescence intensity of the cells dyed by PI. The lower left quadrant shows the viable cells, the upper left shows necrotic cells, the lower right shows the early apoptotic cells; while the upper right shows late apoptotic cells.

As we know, necrosis is a form of traumatic cell death that results from acute cellular injury; while apoptosis is a highly regulated and controlled process that confers advantages during an organism's lifecycle. Unlike necrosis, apoptosis produces cell fragments called apoptotic bodies that phagocytic cells are able to engulf and quickly remove before the contents of the cell can spill out onto surrounding cells and cause damage to the neighboring cells. An early marker of apoptosis is the exposition of phosphatidylserine on the cell surface, whereas it is normally concentrated in the luminal layer of the cytoplasmic membrane [19]. **D-P-4** hybrid promoted greater early apoptosis/necrosis than both monomers and the combination, implying different anti-cancer mechanism compared with them.

3.3. Cell cycle analysis of *DMXAA*, pyranoxanthone, the combination, and **D-P-4**

To establish whether **DMXAA (D)**, pyranoxanthone (**P**), the combination (**D+P** in 1:1 mol ratio), and **D-P-4** inhibited cell growth by interrupting the cell cycle progress, cellular DNA was analyzed and stained with propidium iodide (PI). The cells were analyzed using flow cytometry. The profiles were shown in **Fig. 4**. Obviously, compared with the control group, an increase in the S population was observed in HepG-2 cells after the treatment with **D**, **P**, **D+P**, and **D-P-4** at the dose of 0.2 μ M, respectively. **D-P-4** showed the most capability to arrest cells at S state. It increased S population by 90% compared to the control.

This fact suggests that the cell cycle arrest is one of the primary mechanisms responsible for the anticancer activities of **D**, **P**, **D+P**, and **D-P-4**. The **D-P-4** hybrid alters the manner of cell cycle arrest to S state greater than both monomers and the combination. This may possibly be one reason for the anti-cancer activity enhancement of the hybrid.

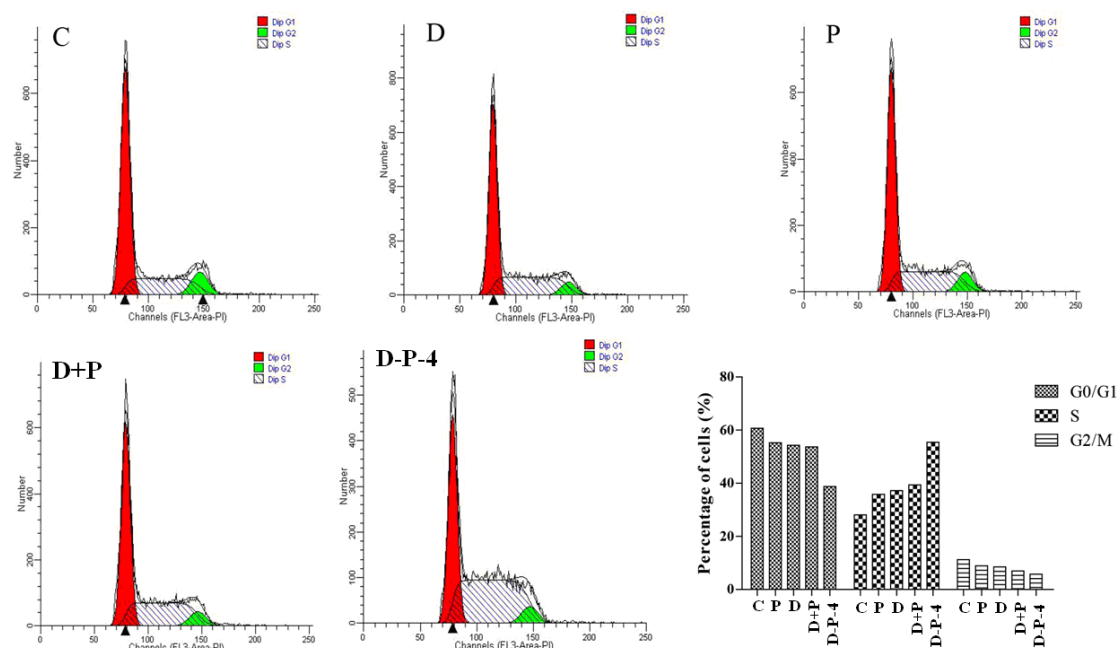


Fig. 4. Cell cycle analysis of HepG-2 cells exposed to **DMXAA (D)**, pyranoxanthone (**P**), the combination (**D+P** in 1:1 mol ratio), and **D-P-4**, respectively. HepG-2 cells were pre-treated with **D**, **P**, **D+P**, and **D-P-4** at a dose of 0.2 μ M, respectively for 24 h. **C** was the control group, without addition of any tested compounds. Cells were collected, fixed in 70% ethanol, and stained with propidium iodide solution. G0/G1: quiescent state/growth phase; S: initiation of DNA replication; G2/M: biosynthesis/mitosis phases.

Usually, the ensuing S phase starts when DNA synthesis commences; when this phase is complete, all of the chromosomes have been replicated, i.e., each chromosome has two (sister) chromatids. If DNA can not be replicated, cell cycle will be stopped at this stage. Based on the current result, it was suggested that **D-P-4** may inhibit the DNA replication and make the cell cycle stop in S phase.

3.4. Influence on the expression levels of proteins related to cell death by pyranoxanthone (**P**), the combination and **D-P-4** hybrid

Cell death includes apoptosis and necrosis. In order to disclose how pyranoxanthone (**P**), the combination (**D+P** in 1:1 mol ratio) and **D-P-4** induced cell apoptosis, we examined the expression levels of caspase-3, cleaved caspase-3, caspase-9, cleaved caspase-9, and cleaved poly (ADP-ribose) polymerase (PARP) by Western Blotting. We found that **P**, **D+P**, and **D-P-4** decreased the levels of caspase-3, and caspase-9, respectively; while in the mean time increased the expression of

cleaved caspase-3 and cleaved PARP (**Fig. 5 I-II**). Of notice, **D+P** and **D-P-4** increased the ratios of cleaved caspase-3(9)/caspase-3(9) and the expression level of cleaved PARP greater than **P** monomer. It was found that **D-P-4** had the greatest effect. As we know, caspase-3 is involved in the apoptotic process, where it is responsible for chromatin condensation and DNA fragmentation [20]. Caspase-9 is an initiator caspase [21]. The initiated caspase-9 will go on to cleave procaspase-3 and procaspase-7. In other hand, PARP is a family of proteins involved in a number of cellular processes involving mainly DNA repair and programmed cell death [22]. When PARP is cleaved by enzymes such as caspases or cathepsins, typically the function of PARP is inactivated. Therefore, these data support that **P**, **D+P**, and **D-P-4** induce cell apoptosis via the adjustment of caspase 3, caspase 9, and PARP, which closely participate in programmed cell death. **D-P-4** hybrid has better effect than pyranoxanthone monomer or the combination.

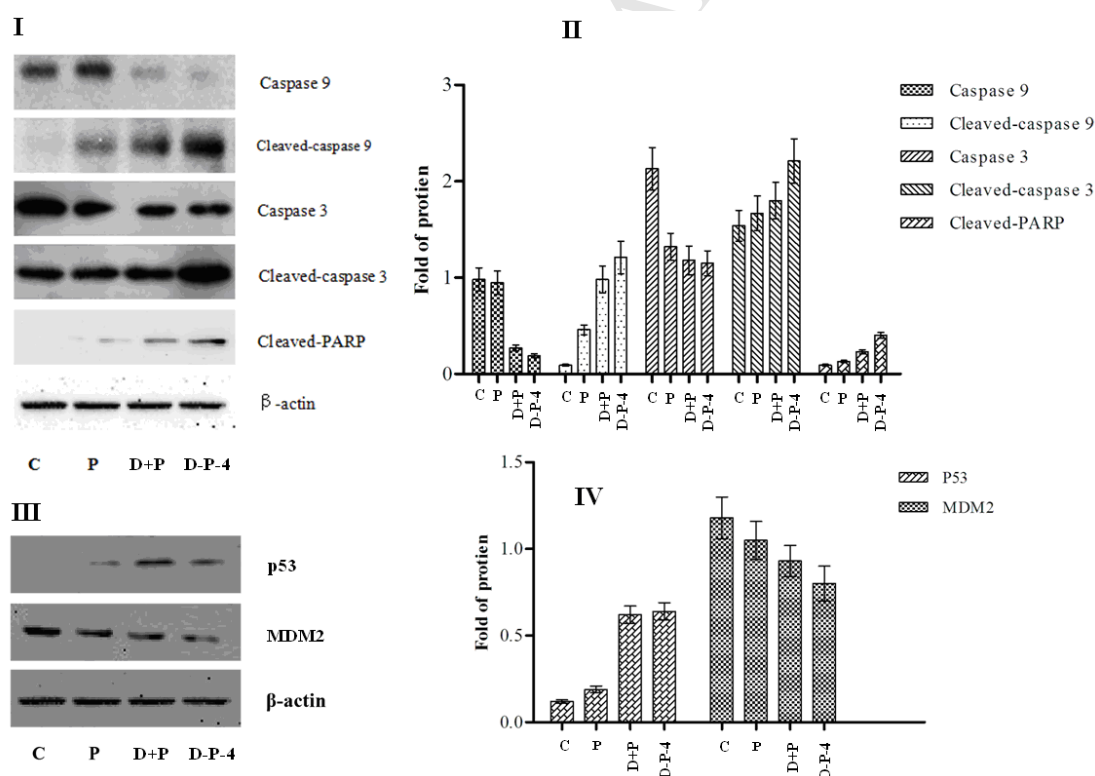


Fig. 5. Effect of **pyranoxanthone (P)**, the combination (**D+P**) and **D-P-4** on proteins related to cell death. HepG-2 cells were treated with **P**, **D+P** (in 1:1 mol ratio), and **D-P-4** at a dose of 0.2 μ M, respectively for 24 h. **C** was the control group, without addition of any tested compounds. The proteins expression levels were measured using Western Blot. The density of each lane was presented as mean \pm standard deviation (SD) for at least three individual experiments. Blots were quantified using Image J software.

We noticed the fact that pyranoxanthone was reported as a putative small-molecule inhibitor of p53/MDM2 interaction [23], in which p53 is a tumor suppressor which plays many roles including the ability to induce cell cycle arrest, DNA repair, senescence, and apoptosis [24,25]; while MDM2 (murine double minute 2) is the main endogenous negative regulator. This oncoprotein MDM2 binds p53 and negatively regulates p53 activity by direct inhibition of p53 transcriptional activity and enhancement of p53 degradation via the ubiquitin-proteasome pathway [26-28]. By inhibiting the p53/MDM2 interaction to restore p53 activity represents an appealing therapeutic strategy for many wild-type p53 tumors with over expressed MDM2. Therefore, we are interested in whether the combination **D+P** and **D-P-4** hybrid can regulate the p53/MDM2 interaction.

To our expect, it was found that **P**, **D+P**, and **D-P-4** up-regulated p53 expression, respectively; while in the other hand, they down-regulated MDM2 expression, respectively (**Fig. 5 III-IV**). Obviously, the combination and **D-P-4** showed the greater activity on the regulation of p53/MDM2 than the **P** monomer, which make these two proteins in a better healthy state. And **D-P-4** had the greatest effect, it changed the p53/MDM2 ratio from 0.083 (control group) to 0.81; while the ratio was 0.67 and 0.19 for **D+P** and **P** group, respectively. This positive effect might be the key mechanism of how **D+P** and **D-P-4** induce cancer cell death. It might conclude based on this evidence that the regulation of p53/MDM2 to a better healthy state is probably the main reason for the synergetic effect in the form of combination or hybrid between pyranoxanthone and **DMXAA**.

3.5. Pyranoxanthone, the combination, and D-P-4 influence Bcl-2 signaling pathway

The mitochondrial pathway plays a significant role in the apoptotic modulation as a major signaling pathways [29]. The mitochondrial-mediated apoptotic pathway can be triggered by several factors, including the expression of B-cell lymphoma 2 (Bcl-2) family members such as Bcl-2, Bcl-2 associated protein X (Bax), B-cell lymphoma-extra large (Bcl-xL) and BH3 interacting-domain death agonist (Bid), which BH

means Bcl-2 homology. There are four BH domains named BH1, BH2, BH3, and BH4. This proteins family can affect the permeability of the mitochondrial membrane and trigger the opening of the mitochondrial permeability transition pore in the inner mitochondrial membrane, resulting in the release of cytochrome c and mitochondrial dysfunction [30].

In the current study, the down-regulation of anti-apoptotic protein Bcl-2 and Bcl-xL, and up-regulation of the pro-apoptotic protein Bax and Bid were observed after the treatment of 0.2 μ M of pyranoxanthone (**P**), the combination **D+P** and **D-P-4** hybrid in **Fig. 6**. Usually, the greater of Bax/Bcl-2 ratio, the more percentage of cell apoptosis is involved. **D-P-4** hybrid showed the greatest activity in regulating the Bax/Bcl-2 ratio, in which it changed the ratio from 0.23 (the control group) to 0.87; while the ratios were 0.58 (**D+P** group) and 0.36 (**P** group), respectively. This evidence indicated that treatment of **P**, **D+P**, and **D-P-4**, respectively against HepG2 cells induce increased apoptosis via the mitochondrial-mediated apoptotic pathway. **D+P** and **D-P-4** showed better activity than **P** monomer, and the hybrid had the best activity.

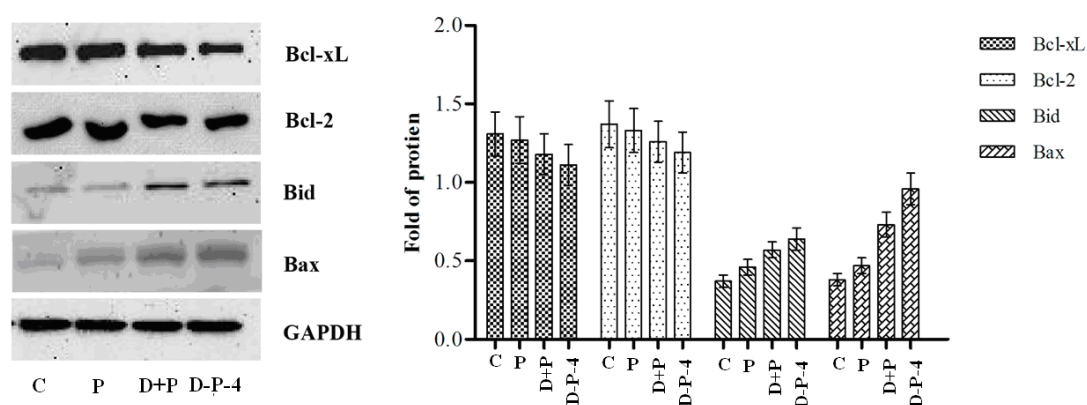


Fig. 6. Effect of **pyranoxanthone (P)**, the combination (**D+P**) and **D-P-4** on proteins related to Bcl-2 signaling pathway. HepG-2 cells were treated with **P**, **D+P** (in 1:1 mol ratio), and **D-P-4** at a dose of 0.2 μ M, respectively for 24 h. **C** was the control group, without addition of any tested compounds. The proteins expression levels were measured using Western Blot. The density of each lane was presented as mean \pm standard deviation (SD) for at least three individual experiments. Blots were quantified using Image J software.

Moreover, the increased expressions of Bid and decreased expressions of Bcl-xL can also lead to the same conclusion as Bax/Bcl-2.

Generally, cancer can be seen as a disturbance in the homeostatic balance between cell growth and cell death. It is of notice that simultaneous over-expression of Bcl-2 and the proto-oncogene myc may produce aggressive B-cell malignancies including lymphoma [31]. In follicular lymphoma, a chromosomal translocation commonly occurs between the fourteenth and the eighteenth chromosomes-t (14 and 18), which places the Bcl-2 gene from chromosome 18 next to the immunoglobulin heavy chain locus on chromosome 14. This fusion gene is deregulated, leading to the transcription of excessively high levels of Bcl-2 [32], and decreases the propensity of these cells for apoptosis. Therefore, targeted or selective inhibited against Bcl-2 can be an effective strategy to treat cancer. Several drugs including G3139, ABT-199, and ABT-263 have been in clinical trial [34-35]. From this viewpoint, **D-P-4** is certainly an promising anti-cancer agent.

4. Conclusions

In a word, four DMXAA (**D**) and pyranoxanthone (**P**) hybrids (**D-P-n**, n = 1-4) were design-synthesized based on multi-target-addressed ligand strategy. Their anticancer activities against four human cells, MCF-7, MDA-MB-231, Hep-G2, and K562 cell lines were evaluated. All the hybrids and the combination (**D+P** in 1:1 mol ratio) exhibited greater inhibitory activities against the four tested cancer cell lines growth with IC₅₀ values between 0.2 and 52 μM. The **D-P-4** hybrid demonstrated the most potent inhibitory activity against MCF-7 and HepG-2 cell lines with IC₅₀ values of 0.534 ± 0.043, and 0.216 ± 0.031 μM, respectively.

The study of structure-activity relationship indicated that the length of carbon chain between **D** and **P** is very important for the inhibitory activity, which in the current study, the optimal carbon chain is 6. It was found that **P** enhanced the inhibitory activity of **D**. The combination of **D** and **P** in 1:1 mol ratio mixture increased 3-5 times the activity against the tested four cell lines growth than **D** itself.

At the same dose of 0.2 μM, **D**, **P**, the combination (**D+P** in 1:1 mol ratio) and **D-P-4** hybrid induced HepG-2 cells apoptosis. The contribution of early apoptosis, necrosis, and late apoptosis were different among both monomers, the combination

and the hybrid. **D-P-4** showed the highest total apoptosis/necrosis rate, and caused far more early apoptosis/necrosis rate than the others. Cell cycle analysis indicated that **D**, **P**, **D+P** and **D-P-4** all arrested more cells on S phase, in which the hybrid showed the greatest effect. Results in Western Blot indicated that **P**, **D+P**, and **D-P-4** decreased the expression levels of caspase 3, caspase 9, and MDM2; while in the mean time increased the expression levels of cleaved-caspase 3, cleaved-caspase-9, cleaved-PARP, and p53. The hybrid showed the best regulation of p53/MDM2 to a better healthy state, in which the p53/MDM2 ratio was 0.81 compared 0.083 for the control.

P, **D+P**, and **D-P-4**, respectively showed another activity to decrease Bcl-2 and Bcl-xL expression levels, while in the mean time increase the expression levels of Bax and Bid, indicating the ability to improve cancer cell apoptosis through Bcl-2 signaling pathway. **D-P-4** again had the best activity to adjust the Bcl-2 protein family, in which the Bax/Bcl-2 ratio was 0.87 compared 0.23 for the control. Better improvement on p53/MDM2 and Bax/Bcl-2 might be the possible reasons for the synergistic effect in the form of hybrid between **D** and **P**. All the evidences support that **D-P-4** hybrid is a better anticancer therapy with multi-target function.

5. Experimental section

5.1. Materials

All chemicals salicylic acids and phenolics were purchased from Aldrich or Adamas without further purification. Silica gel for column chromatography was purchased from Qingdao Marine Chemicals Inc, China. Chromatographic grade methanol was bought from Shandong YuWang Reagent Company (China).

The human CML cell line MDA-MB-231 and MCF-7, Hep-G2, and K562 were obtained from the Cell Bank of the Chinese Academy of Sciences (Shanghai, China). MDA-MB-231 and MCF-7 cells were cultured in RPMI 1640 medium (Life Technologies, Grand Island, NY, USA). HL-7702 and NIH/3T3 cells were grown in DMEM medium (Life Technologies, Grand Island, NY, USA).

The reagents PI and JC-1 were purchased from Sigma Chemical Co. (St. Louis, MO, USA). Pierce™ BCA Protein Assay Kit was obtained from Thermo Fisher Scientific

(Rockford, IL, USA). MTT, TUNEL Apoptosis Detection Kit, dithiothreitol (DTT), Nuclear and Cytoplasmic Extraction Kit, RIPA buffer and RNase were purchased from Beyotime (Shanghai, China). Phosphatase inhibitor cocktail tablets and protease inhibitor cocktail tablets were supplied by Roche (Mannheim, Germany). All other chemicals and solvents were of reagent or HPLC grade.

β -Actin, GADPH, caspase 3, caspase 9, cleaved-caspase 3, cleaved-caspase 9, cleaved PARP, Bax, Bid, Bcl-2, Bcl-xL, anti-mouse, and anti-rabbit horseradish peroxidase-conjugated secondary antibodies were purchased from Cell Signaling Technology (CST, Beverly, MA, USA).

5.2. Synthetic process

5.2.1. General chemical experimental procedures

Nuclear Magnetic Resonance (NMR) spectra were recorded on either a Bruker AV-300 or a Bruker AV-400, or a Bruker AV-500 (Bruker Biospin, Swiss). Tetramethylsilicane (TMS) was used as an internal standard. ESI-MS were recorded on a Finnigan LCQ Advantage MAX mass spectrometer. HPLC was performed on either a LC-100 liquid chromatograph equipped with a tunable LC-100 UV detector (Shanghai Wufeng Inc., China) or an Agilent 1200 series liquid chromatograph equipped with an Agilent 1200 Series UV detector (Agilent Technologies, USA). Columns used were Cosmosil 5C₁₈ (Nacalai Tesque Inc., Japan) for general purification. Pre-coated thin-layer chromatography (TLC) plates (Institute of Yantai Chemical Industry, China) were used for TLC. Spots on TLC plates were detected by either a ZF-7A portable UV detector or spraying Bismuth potassium iodide solution followed subsequent heating. Ethanol was refluxed over Fresh magnesium ribbon for 5 hours and redistilled.

5.2.2. Synthesis of 5,6-dimethylxanthone-4-acetic acid (DMXAA)

The synthesis was carried on referred to a procedure described in literature [17]. Firstly, 3,4-dimethylbenzoic acid was turned into 2,5-dibromo-3,4-dimethylbenzoic

acid, which was named as compound **1**. Compound **1** was then converted into its potassium salt and dried thoroughly. This salt reacted with the anhydrous disodium salt of 2-hydroxyphenylacetic acid under the interaction of tris[2-(2-methoxyethoxy)ethyl]amine (TDA-1) and copper (I) to give 7-bromo-5,6-dimethyl-9-oxo-9H-xanthen-4-yl acetic acid (**2**). Hydrogenation of compound **2** gave **DMXAA** in an overall yield of 51% in four steps. Purity 98.5%. ^1H NMR (DMSO- d_6 , 300 MHz) δ : 12.62 (s, 1H), 8.10 (dd, $J = 8.0, 1.6$ Hz, 1H, H-1), 7.93 (d, $J = 8.4$ Hz, 1H, H-8), 7.79 (dd, $J = 7.2, 1.6$ Hz, 1H, H-3), 7.42 (dd, $J = 7.6, 1.6$ Hz, 1H, H-7), 7.31 (d, $J = 8.0$ Hz, 1H, H-2), 3.99 (s, 2H), 2.44 (s, 3H), 2.42 (s, 3H); ^{13}C NMR (DMSO- d_6 , 75 MHz) δ : 176.1 (-COOH), 171.7 (C-9), 153.7 (C-4a), 153.2 (C-4b), 144.6 (C-6), 136.5 (C-3), 125.9 (C-4), 125.2 (C-5), 125.1 (C-7), 124.6 (C-1), 123.6 (C-2), 122.5 (C-8), 120.5 (C-8b), 118.7 (C-8a), 35.4 (C-9), 20.1 (CH_3), 11.0 (CH_3); MS-ESI m/z : 283.2 $[\text{M}+\text{H}]^+$.

5.2.3. Synthesis of 12-O-(*n*-hydroxyalkyl)pyranoxanthenes

5.2.3.1. Synthesis of 3,4-dihydroxy-9H-xanthen-9-one

To a 50-ml flask, 8 ml phosphorus oxychloride (POCl_3) and anhydrous zinc chloride (6.8 g, 0.05 mol) were added. The suspension was stirred at 70°C until ZnCl_2 was completely dissolved into phosphorus oxychloride. The mixture was then cooled down to room temperature (r.t.). Afterwards, salicylic acid (0.138 g, 1.0 mmol) and pyrogallol (0.151 g, 1.2 mmol) were added. Then the mixture was heated with microwave reactor with a programmed procedure of 75°C for 30 min. Afterwards, the mixture was cooled down to r.t. and pulled into ice water stirring for 20 min. The mixed solution was filtered, washed with cold water. The solid residues were collected and purified by flash column liquid chromatography led to yellow powder 0.176 g, yield 77.1%. M.p. 220~221 °C; ^1H NMR (DMSO- d_6 , 300 MHz) δ : 7.38 (td, $J = 8.1, 0.9$ Hz, 1H, H-8), 7.29 (dd, $J = 8.1, 0.9$ Hz, 1H, H-6), 6.91-6.95 (m, 2H, H-5, 7), 6.89 (d, $J = 8.4$ Hz, 1H, H-1), 6.36 (d, $J = 8.4$ Hz, 1H, H-2); ^{13}C NMR (DMSO- d_6 , 75 MHz) δ : 202.62 (C-9), 157.41 (C-4b), 153.61 (C-3), 153.24 (C-4a), 133.64 (C-6), 133.54 (C-4), 131.06 (C-8), 127.04 (C-7), 126.18 (C-8a), 120.03 (C-1), 117.66 (C-5),

115.24 (C-8b), 108.41 (C-2); MS-ESI m/z : 228.2 [M+H]⁺.

5.2.3.2. Synthesis of pyranoxanthone

To a 50-ml flask, 20 ml chloroform, 3,4-dihydroxy-9*H*-xanthen-9-one (0.228 g, 1.0 mmol), and montmorillonoid K10 (4.5 g, 20 eg) were added. The mixture was radiated with a microwave reactor at 600 W under stirring for 40 min. After the end of reaction, montmorillonoid K10 was filtered and washed. All the filtration was combined. Removal of solvent was carried on by rotary evaporation under reduced pressure. The solid residues were collected and purified by flash column liquid chromatography led to slight yellow powder 0.13 g, yield 38.5%, Purity 97.6%. M.p. 176~178 °C; ¹H NMR (400 MHz, CDCl₃) δ : 8.33 (1H, dd, J = 8.0 and 1.6 Hz, H-7), 7.70 (1H, ddd, J = 7.7, 8.0, 1.6 Hz, H-9), 7.70 (1H, s, H-5), 7.58 (1H, dd, J = 8.0, 1.0 Hz, H-8), 7.35 (1H, ddd, J = 7.3, 7.3, 1.0 Hz, H-10), 5.74 (1H, br s, OH), 2.93 (2H, t, J = 6.7 Hz, H-4), 1.92 (2H, t, J = 6.7 Hz, H-3), 1.43 (6H, s, 2 -CH₃); ¹³C-NMR (75 MHz, CDCl₃) δ : 176.72 (C-6), 156.21 (C-10a), 146.33 (C-12a), 143.24 (C-11a), 134.30 (C-9), 132.42 (C-12), 126.60 (C-7), 123.62 (C-8), 121.53 (C-6a), 118.22 (C-10), 117.93 (C-5), 117.04 (C-4a), 115.41 (C-5a), 76.54 (C-2), 32.66 (C-3), 27.02 (C-4), 21.74 (C-1'); ESI-MS (m/z): 297.2[M+H]⁺.

5.2.3.3. Synthesis of 3,4-dihydro-12-*O*-(3'-hydroxypropyl)-2,2-dimethyl-2*H*,6*H*-pyrano[3,2-*b*]xanthen-6-one (P-1)

To a 50-ml flask, pyranoxanthone (0.296 g, 1.0 mmol) and NaOH (44 mg, 1.1 mmol) in 15 ml of dried DMF. 3-Bromopropanol (0.208 g, 1.5 mmol) in 5 ml dried DMF was then added dropwise with stirring. The reaction was lasted at r. t. for 24 h. After the finish of reaction, the mixture was pulled into 50 ml ice-water with violently stirring for 20 min. The precipitates were collected by filtrate, and were purified by flash column liquid chromatography led to slight yellow powder 0.318 g, yield 89.6%. M.p.: 161-163 °C; ¹H-NMR (CDCl₃, 400 MHz) δ : 8.35 (1H, dd, J = 8.0 and 1.6 Hz, H-8), 7.73 (1H, ddd, J = 7.6, 8.0, 1.6 Hz, H-6), 7.71 (1H, s, H-1), 7.60 (1H, dd, J = 8.0 and 1.0 Hz, H-5), 7.37 (1H, ddd, J = 7.6, 7.6, and 1.0 Hz, H-4), 5.76 (1H, s, OH),

4.21 (2H, t, $J = 2.6$ Hz, H-1"), 3.57 (2H, t, $J = 2.6$ Hz, H-3"), 2.95 (4H, m, H-2', 2"), 1.97 (2H, t, $J = 2.6$ Hz, H-1'), 1.43 (6H, s, H-4', 5'). $^{13}\text{C-NMR}$ (CDCl_3 , 100 MHz) δ : 177.19 (C-9), 157.31 (C-4b), 147.32 (C-3), 144.27 (C-4a), 135.37 (C-4), 133.47 (C-6), 127.62 (C-8), 124.65 (C-7), 122.57 (C-1), 119.25 (C-8a), 118.95 (C-2), 118.05 (C-5), 116.44 (C-8b), 75.59 (C-3'), 62.45 (C-1"), 57.11 (C-3"), 32.75 (C-2'), 31.24 (C-2"), 26.44 (C-4'), 26.44 (C-5'), 22.62 (C-1'). MS-ESI m/z : 355.16 $[\text{M}+\text{H}]^+$.

5.2.3.4. Synthesis of 3,4-dihydro-12-O-(4'-hydroxybutyl)-2,2-dimethyl-2H,6H-pyrano[3,2-b]xanthen-6-one (**P-2**)

Followed the same procedure described in 5.2.3.3. Led to light yellow powder 0.37 g, yield 83.4%. M.p.: 159-161 °C, $^1\text{H-NMR}$ (CDCl_3 , 400 MHz) δ : 8.31 (1H, dd, $J = 8.0$ and 1.6 Hz, H-8), 7.70 (1H, ddd, $J = 7.6$, 8.0, 1.6 Hz, H-6), 7.63 (1H, s, H-1), 7.52 (1H, dd, $J = 8.0$ and 1.0 Hz, H-5), 7.31 (1H, ddd, $J = 7.6$, 7.6, and 1.0 Hz, H-4), 5.70 (1H, s, OH), 4.15 (2H, t, $J = 2.6$ Hz, H-1"), 3.43 (2H, t, $J = 2.6$ Hz, H-4"), 2.91 (6H, m, H-2', 2", 3"), 2.02 (2H, t, $J = 2.6$ Hz, H-1'), 1.40 (6H, s, H-4', 5'). $^{13}\text{C-NMR}$ (CDCl_3 , 100 MHz) δ : 178.11 (C-9), 158.38 (C-4b), 148.35 (C-3), 145.48 (C-4a), 136.40 (C-4), 134.39 (C-6), 128.72 (C-8), 125.70 (C-7), 123.87 (C-1), 120.15 (C-8a), 119.44 (C-2), 119.15 (C-5), 117.43 (C-8b), 76.88 (C-3'), 63.49 (C-1"), 58.13 (C-4"), 33.87 (C-2'), 32.75 (C-2"), 31.64 (C-3"), 27.43 (C-4'), 27.43 (C-5'), 23.65 (C-1'). MS-ESI m/z : 369.18 $[\text{M}+\text{H}]^+$.

5.2.3.5. Synthesis of 3,4-dihydro-12-O-(5'-hydroxypentyl)-2,2-dimethyl-2H,6H-pyrano[3,2-b]xanthen-6-one (**P-3**)

Followed the same procedure described in 5.2.3.3. Led to light yellow powder 0.327 g, yield 85.6%. M.p.: 155-157 °C; $^1\text{H-NMR}$ (CDCl_3 , 400 MHz) δ : 8.37 (1H, dd, $J = 8.0$ and 1.6 Hz, H-8), 7.76 (1H, ddd, $J = 7.6$, 8.0, 1.6 Hz, H-6), 7.69 (1H, s, H-1), 7.57 (1H, dd, $J = 8.0$ and 1.0 Hz, H-5), 7.38 (1H, ddd, $J = 7.6$, 7.6, and 1.0 Hz, H-4), 5.76 (1H, s, OH), 4.19 (2H, t, $J = 2.6$ Hz, H-1"), 3.48 (2H, t, $J = 2.6$ Hz, H-5"), 2.96 (8H, m, H-2', 2", 3", 4"), 2.07 (2H, t, $J = 2.6$ Hz, H-1'), 1.45 (6H, s, H-4', 5'); $^{13}\text{C-NMR}$ (CDCl_3 , 100 MHz) δ : 178.34 (C-9), 158.57 (C-4b), 148.65 (C-3), 145.59

(C-4a), 136.67 (C-4), 134.58 (C-6), 128.89 (C-8), 125.85 (C-7), 123.92 (C-1), 120.34 (C-8a), 119.68 (C-2), 119.63 (C-5), 117.51 (C-8b), 76.96 (C-3'), 63.67 (C-1''), 58.45 (C-5''), 33.99 (C-2'), 32.94 (C-2''), 31.86 (C-3''), 29.86 (C-4''), 27.66 (C-4'), 27.66 (C-5'), 23.59 (C-1'); MS-ESI m/z : 383.21 [M+H]⁺.

5.2.3.6. Synthesis of 3,4-dihydro-12-O-(6'-hydroxyhexyl)-2,2-dimethyl-2H,6H-pyrano[3,2-b]xanthen-6-one (**P-4**)

Followed the same procedure described in 5.2.3.3. Led to light yellow powder 0.329 g, yield 83.1%. M.p.: 153-155 °C; ¹H-NMR (CDCl₃, 400 MHz) δ : 8.31 (1H, dd, $J = 8.0$ and 1.6 Hz, H-8), 7.72 (1H, ddd, $J = 7.6, 8.0, 1.6$ Hz, H-6), 7.48 (1H, s, H-1), 7.46 (1H, dd, $J = 8.0$ and 1.0 Hz, H-5), 7.54 (1H, ddd, $J = 7.6, 7.6,$ and 1.0 Hz, H-4), 5.56 (1H, s, OH), 4.26 (2H, t, $J = 2.6$ Hz, H-1''), 3.57 (2H, t, $J = 2.6$ Hz, H-6''), 2.92 (10H, m, H-2', 2'', 3'', 4'', 5''), 2.11 (2H, t, $J = 2.6$ Hz, H-1'), 1.41 (6H, s, H-4', 5'); ¹³C-NMR (CDCl₃, 100 MHz) δ : 179.02 (C-9), 158.90 (C-4b), 149.25 (C-3), 145.93 (C-4a), 137.33 (C-4), 135.08 (C-6), 129.31 (C-8), 126.22 (C-7), 124.38 (C-1), 120.80 (C-8a), 119.95 (C-2), 119.97 (C-5), 117.96 (C-8b), 77.89 (C-3'), 64.32 (C-1''), 58.96 (C-6''), 34.62 (C-2'), 32.41 (C-2''), 31.49 (C-3''), 29.67 (C-4''), 28.48 (C-4'), 27.53 (C-4'), 27.53 (C-5'), 22.97 (C-1'); MS-ESI m/z : 397.23 [M+H]⁺.

5.2.4. Synthesis of DMXAA-pyranoxanthone hybrids

5.2.4.1. Synthesis of 3,4-dihydro-2,2-dimethyl-2H,6H-pyrano[3,2-b]xanthen-6-one-12-O-propyl 5,6-dimethylxanthone-4-acetate (**D-P-1**)

To a 100-ml flask, DMXAA (0.339 g, 1.2 mmol), DCC (0.248 g, 1.2 mmol) and DMAP (15 mg, 0.12 mmol) were dissolved in 30 ml dried DMF. Compound P-1 (0.354 g, 1.0 mmol) in 10 ml dried DMF was then added dropwise with stirring. The reaction was lasted at r. t. for 24 h. After the finish of reaction, the mixture was pulled into 50 ml ice-water with violently stirring for 20 min. The precipitates were collected by filtrate, and were purified by flash column liquid chromatography led to white powder 0.324 g, yield 52.4%, purity 97.4%. Mp: 205-206 °C; ¹H NMR (DMSO-*d*₆, 500 MHz) δ : 8.01-8.04 (m, 3H, H-1, 7', 9'), 6.85-6.87 (m, 3H, H-3, 8, 10'), 6.73-6.75

(m, 2H, H-5', 8'), 6.28-6.31 (m, 1H, H-2), 6.21-6.24 (m, 1H, H-7), 4.00-4.03 (m, 2H, H-5''), 3.98 (m, 2H, H-3''), 3.71 (s, 2H, H-1''), 3.34-3.36 (m, 2H, H-4''), 2.76-2.79 (m, 2H, H-4'), 2.62-2.64 (m, 2H, H-3'), 1.78-1.81 (s, 6H, 5,6-CH₃), 1.41-1.44 (s, 6H, 2'-CH₃); ¹³C NMR (DMSO-*d*₆, 125 MHz) δ : 181.36 (C-9), 179.08 (C-6'), 176.54 (C-2''), 166.76 (C-11a'), 164.13 (C-4b), 161.70 (C-10a'), 158.32 (C-3), 156.63 (C-4a), 151.97 (C-9'), 136.51 (C-4), 135.63 (C-6), 134.17 (C-12a'), 129.89 (C-12'), 128.48 (C-8), 127.48 (C-10'), 126.45 (C-8'), 125.63 (C-9'), 125.45 (C-7), 124.63 (C-4a'), 124.19 (C-5'), 123.39 (C-7'), 122.09 (C-5a'), 121.23 (C-8a), 118.20 (C-2), 104.48 (C-6a'), 98.03 (C-5), 93.83 (C-8b), 79.88 (C-2'), 68.93 (C-5''), 64.24 (C-3''), 34.07 (C-1''), 33.98 (C-3'), 32.85 (C-4'), 28.32 (C-4''), 25.17 (2 \times 2'-CH₃), 18.65 (6-CH₃), 16.43 (5-CH₃); MS-ESI *m/z*: 619.23 [M+H]⁺; HRMS (*m/z*): calc. for [C₃₈H₃₄O₈+H]⁺ 619.2332, found 619.2338.

5.2.4.2. Synthesis of 3,4-dihydro-2,2-dimethyl-2H,6H-pyrano[3,2-*b*]xanthen-6-one-12-*O*-butyl 5,6-dimethylxanthone-4-acetate (**D-P-2**)

Followed the same procedure described in 5.2.4.1. Led to 0.324 g, yield 51.3%, purity 98.4%. M. p.: 209-211 °C; ¹H NMR (DMSO-*d*₆, 500 MHz) δ : 8.13-8.16 (m, 3H, H-1,7', 9'), 6.96-6.99 (m, 3H, H-3, 8, 10'), 6.81-6.87 (m, 2H, H-5', 8'), 6.40-6.44 (m, 1H, H-2), 6.31-6.36 (m, 1H, H-7), 4.13 (m, 2H, H-6''), 4.10 (m, 2H, H-3''), 3.74 (s, 2H, H-1''), 3.49-3.429 (m, 2H, H-5''), 3.03-3.08 (m, 2H, H-4''), 2.81-2.86 (m, 4H, H-3', 4'), 1.90-1.95 (s, 6H, 5,6-CH₃), 1.51-1.56 (s, 6H, 2'-CH₃); ¹³C NMR (DMSO-*d*₆, 125 MHz) δ : 182.23 (C-9), 179.95 (C-6'), 177.41 (C-2''), 167.63 (C-11a'), 165.00 (C-4b), 162.57 (C-10a'), 159.19 (C-3), 157.50 (C-4a), 152.84 (C-9'), 137.38 (C-4), 136.50 (C-6), 135.04 (C-12a'), 130.76 (C-12'), 129.35 (C-8), 128.35 (C-10'), 127.33 (C-8'), 126.50 (C-9'), 126.32 (C-7), 125.50 (C-4a'), 124.26 (C-5'), 122.96 (C-7'), 122.68 (C-5a'), 122.10 (C-8a), 119.08 (C-2), 105.35 (C-6a'), 98.91 (C-5), 94.70 (C-8b), 80.75 (C-2'), 69.80 (C-6''), 65.11 (C-3''), 34.94 (C-1''), 34.85 (C-3'), 33.72 (C-5''), 33.37 (C-4''), 26.23 (2'-CH₃), 26.04 (2'-CH₃), 16.88 (6-CH₃), 14.69 (5-CH₃); MS-ESI *m/z*: 633.22 [M+H]⁺; HRMS (*m/z*): calc. for [C₃₉H₃₆O₈+H]⁺ 633.2488, found 633.2492.

5.2.4.3. *Synthesis of 3,4-dihydro-2,2-dimethyl-2H,6H-pyrano[3,2-b]xanthen-6-one-12-O-pentyl 5,6-dimethylxanthone-4-acetate (D-P-3)*

Followed the same procedure described in 5.2.4.1. Led to white powder 0.32 g, yield 49.6%, purity 99.2%. M. p.: 211-213°C; ¹H NMR (DMSO-*d*₆, 500 MHz) δ: 8.15-8.11 (m, 3H, H-1, 7', 9'), 6.97-6.94 (m, 3H, H-3, 8, 10'), 6.86-6.81 (m, 2H, H-5', 8'), 6.45-6.41 (m, 1H, H-2), 6.36-6.32 (m, 1H, H-7), 4.10 (m, 2H, H-7''), 4.07 (m, 2H, H-3''), 3.72 (s, 2H, H-1''), 3.46-3.41 (m, 2H, H-6''), 2.99-2.95 (m, 4H, H-3', 4''), 2.87-2.92 (m, 4H, H-4', 5''), 1.90-1.95 (s, 6H, 5,6-CH₃), 1.50-1.54 (s, 6H, 2'-CH₃); ¹³C NMR (DMSO-*d*₆, 125 MHz) δ: 182.95 (C-9), 180.67 (C-6'), 178.14 (C-2''), 168.35 (C-11a'), 165.72 (C-4b), 163.30 (C-10a'), 159.92 (C-3), 158.22 (C-4a), 153.56 (C-9'), 138.10 (C-4), 137.23 (C-6), 135.76 (C-12a'), 131.48 (C-12'), 130.08 (C-8), 129.07 (C-10'), 128.05 (C-8'), 127.22 (C-9'), 127.04 (C-7), 126.23 (C-4a'), 125.79 (C-5'), 124.99 (C-7'), 123.68 (C-5a'), 122.83 (C-8a), 119.80 (C-2), 106.08 (C-6a'), 99.63 (C-5), 95.42 (C-8b), 81.47 (C-2'), 70.52 (C-7''), 65.83 (C-3''), 35.66 (C-1''), 35.57 (C-3'), 34.44 (C-4'), 29.92 (C-6''), 26.95 (C-4''), 26.76 (C-5''), 26.76 (2×2'-CH₃), 17.61 (6-CH₃), 15.42 (5-CH₃); MS-ESI *m/z*: 647.28 [M+H]⁺; HRMS (*m/z*): calc. for [C₄₀H₃₈O₈+H]⁺ 647.2645, found 647.2642.

5.2.4.4. *Synthesis of 3,4-dihydro-2,2-dimethyl-2H,6H-pyrano[3,2-b]xanthen-6-one-12-O-hexyl 5,6-dimethylxanthone-4-acetate (D-P-4)*

Followed the same procedure described in 5.2.4.1. Led to white powder 0.319 g, yield 48.3%, purity 98.8%. M.p.: 215-217°C; ¹H NMR (DMSO-*d*₆, 500 MHz) δ: 8.14-8.10 (m, 3H, H-1, 7', 9'), 6.96-6.92 (m, 3H, H-3, 8, 10'), 6.85-6.80 (m, 2H, H-5', 8'), 6.38-6.33 (m, 1H, H-2), 6.35-6.30 (m, 1H, H-7), 4.10 (m, 2H, H-8''), 4.07 (m, 2H, H-3''), 3.76 (s, 2H, H-1''), 3.46-3.44 (m, 4H, H-3', 7''), 2.99-2.95 (m, 4H, H-4'',6''), 2.92-2.86 (m, 4H, H-4', 5''), 1.92-1.88 (s, 6H, 5,6-CH₃), 1.48-1.53 (s, 6H, 2'-CH₃); ¹³C NMR (DMSO-*d*₆, 125 MHz) δ: 183.25 (C-9), 180.98 (C-6'), 178.44 (C-2''), 168.65 (C-11a'), 166.02 (C-4b), 163.60 (C-10a'), 160.22 (C-3), 158.52 (C-4a), 153.86 (C-9'), 138.40 (C-4), 137.53 (C-6), 136.07 (C-12a'), 131.79 (C-12'), 130.38 (C-8),

129.38 (C-10'), 128.35 (C-8'), 127.52 (C-9'), 127.35 (C-7), 126.53 (C-4a'), 126.09 (C-5'), 125.29 (C-7'), 123.98 (C-5a'), 123.13 (C-8a), 120.10 (C-2), 106.38 (C-6a'), 99.93 (C-5), 95.73 (C-8b), 81.78 (C-2'), 70.82 (C-6''), 66.14 (C-3''), 35.96 (C-1''), 35.88 (C-3'), 34.74 (C-8''), 34.40 (C-4''), 29.33 (C-7''), 26.95 (C-6''), 27.25 (C-5''), 26.06 (2×2'-CH₃), 17.91 (6-CH₃), 15.72 (5-CH₃); MS-ESI *m/z*: 661.31 [M+H]⁺; HRMS (*m/z*): calc. for [C₄₁H₄₀O₈+H]⁺ 662.2801, found 661.2805.

5. 3. Biological section

5.3.1. Cell culture

All the cell lines were grown in specific media supplemented with 10% fetal bovine serum (FBS, Gibco), 100 U/ml penicillin and 100 µg/ml streptomycin (Invitrogen, Carlsbad, CA, USA). The cells were grown in a 5% CO₂ humidified atmosphere in incubators maintained at 37°C.

5.3.2. Cell proliferation assay

3-(4,5-cimethylthiazol-2-yl)-2,5-diphenyl tetrazolium bromide (MTT) assay was used to detect inhibition of cellular proliferation mediated by the drugs. This assay was applied to all cell lines. The process was describe below: Cells in suspension were plated in 96-well plates at a density of 5×10³ cells/well and cultured for 24 h. Then the medium was replaced with the respective medium containing drugs at different concentrations and incubated for 24 h. The final DMSO concentration in all experiments was less than 0.1% in medium. The concentration range of tested samples was 0-200 µM and two-fold serial dilutions were applied. Afterwards, 10 µL MTT solution (5 mg/ml) was added to each well, and the plate was incubated for an additional 4 h. The absorbance of the converted dye in living cells was measured at a wavelength of 570 nm using a microplate reader (Bio-Rad; Hercules, CA, USA) after 100 µL of DMSO added. IC₅₀ values were determined by the nonlinear multipurpose curve fitting program GraphPad Prism. All of the tests were repeated at least 3 times.

5.3.3. Apoptosis and necrosis assay

HepG-2 cells (2×10^5 cells/ml) were plated in 6-well plates and then treated with either vehicle or 0.2 μ M of **DMXAA (D)**, pyranoxanthone (**P**), **D+P** in 1:1 mol ratio, and **D-P-4**. The cells were incubated at 37 °C, 5% CO₂ for 24 h. Then the cells were collected by centrifugation at r.t. and washed twice with ice-cold PBS. Afterwards, the cells were suspended in 100 μ L annexin V binding buffer and 5 μ L each of annexin V and PI were added to these samples. Next, these samples were incubated for 30 min at room temperature and then assayed by flow cytometric analysis (FACScan, Becton Dickinson, San Jose, CA). All of the tests were repeated at least 3 times.

5.3.4. Western Blot

HepG-2 cells were collected and washed with PBS after the treatment with 0.2 μ M of **P**, **D+P** (1:1 mol ratio), **D-P-4**, respectively. Then, the cells were lysed with RIPA buffer for 45 min on ice and then centrifuged at 12000 g at 4°C for 15 min. Then the total cellular protein were collected and the nuclear proteins were extracted using a nuclear and cytoplasmic extraction kit. The protein concentration was measured using a BCA protein assay kit. Equal amounts of protein (30 μ g) were separated via 10-15% gradient SDS-PAGE and transferred to PVDF membranes (Millipore, USA). The membranes were blocked with 5% BSA at room temperature for 1 h, incubated with primary antibodies for at least 16 h at 4°C, and then washed and incubated with HRP-conjugated secondary antibodies at room temperature for 1 h. Protein bands were visualized using enhanced chemiluminescence detection reagents (Bio-Rad, USA). The resulting images were scanned using a scanner (Epson V330 Photo, Japan).

5.3.5. Cell cycle assay

HepG-2 cells (2×10^5 cells/ml) were seeded into 6-well plates and treated with vehicle or **D**, **P**, **D+P** (1:1 mol ratio), and **D-P-4** at a dose of 0.2 μ M, respectively for 28 h. Then the cells were collected and washed twice with PBS and fixed in cold 70% ethanol (-20°C) for 12 h. The ethanol were carefully removed by centrifugation and the cells were suspended in 1 ml staining reagent (100 mg RNase+50 mg PI/ml) and kept

in darkness for 40 min at r.t. Cell cycle analysis was tested via a flow cytometry (BD FACS Calibur, Franklin Lakes, CA, USA) with a excitation wavelength at 605 nm.

5.3.6. Stability of **D-P-4**

D-P-4 was dissolve in PBS to be a stock solution with a concentration of 10 μ M/l. Then 1 ml **D-P-4** solution and 4 ml serum (Kunming mice from the animal research center at medical laboratory animal center of Guangdong Province in China) were suspended together for 1 min, and the suspension was put into the incubator at 37°C. At the set time point, 10 μ l sample was taken out, respectively, and pretreated with methanol and perchloric acid 20% to eliminate the proteins. The mixture was centrifuged at 10000 r/min for 5 minutes. Then the supernate was submitted for RP-HPLC analysis. The instrument used was Agilent 1200 (Agilent Co., Germany). Column: COSMOSIL 5C18-MS-II, 4.6 \times 250 mm; Flow rate: 1.0 ml/min; Wavelength: 254 nm; Eluant: methanol : H₂O = 55 : 45 (isocratic).

The content percentage of **D-P-4** was set 100% at 0 h time point. The content percentage at any time point was calculated as following: $A_t/A_0 \times 100\%$, where A_t and A_0 are the peak area at t time point and 0 h time point, respectively. Each experiments was repeated 4 times.

5.3.6. Statistical analysis

All data are expressed as the mean \pm standard deviation (SD) of three independent experiments. Statistical significance was assessed using Student's *t*-test (for comparisons of two treatment groups) or one-way ANOVA (for comparisons of three or more groups). *P*-values < 0.05 were considered statistically significant.

Acknowledgements

This research was financially supported by Guangdong Provincial Project of Science and Technology (No. 2015A030311012), the Guangzhou Project of Science and Technology (No. 201607010215), and the Fundamental Research Funds for the Central Universities (11615323).

References

- [1] N. M. O'Boyle, M. J. Meegan, Designed multiple ligands for cancer therapy, *Curr. Med. Chem.* 18(31) (2011) 4722-4737.
- [2] A. Petrelli, S. Giordano, From single- to multi-target drugs in cancer therapy: When aspecificity becaomes an advantage, *Curr. Med. Chem.* 15(5) (2008) 422-432.
- [3] Y. Hu, L. Zhang, H. Wang, S. Xu, A. Mujeeb, G. Nie, H. Tang, Y. Wang, Biological effects of amphiphilic copolymer nanoparticle-encapsulated multi-target chemotherapeutic drugs on MCF-7 human breast cancer cells, *Metabolomics* 13(5) (2017) 49, **DOI:** 10.1007/s11306-017-1187-x.
- [4] G. Zha, H. Qin, B. G. M. Yourssif, M. W. Muhammad, M. A. G. Raja, A. H. Abdelazeem, S. N. A. Bukhari, Discovery of potential anticancer multi-targeted ligustrazine based cyclohexanone and oxime analogs overcoming the cancer multidrug resistance, *J. Eur. Med. Chem.* 135 (2017) 34-48.
- [5] D. Sunif, P. R. Kamath, Multi-Target Directed Indole Based Hybrid Molecules in Cancer Therapy: An Up-To-Date Evidence-Based Review, *Curr. Topics in Med. Chem.* 17(9) (2017) 959-985.
- [6] Y. Zhou, S. Shan, Z.-B. Li, L.-J. Xin, D.-S. Pan, Q.-J. Yang, Y.-P. Liu, X.-P. Yue, X.-R. Liu, J.-Z. Gao, J.-W. Zhang, Z.-Q. Ning, X.-P. Lu, CS2164, a novel multi-target inhibitor against tumor angiogenesis, mitosis and chronic inflammation with anti-tumor potency, *Cancer Sci.* 108(3) (2017) 469-477.
- [7] J. Yan, Y. Guo, Y. Wang, F. Mao, L. Huang, X. Li, Design, synthesis, and biological evaluation of benzoselenazole-stilbene hybrids as multi-target -directed anti-cancer agents, *J. Eur. Med. Chem.* 95 (2015) 220-229.
- [8] C.-T. Luo, S.-S. Mao, F.-L. Li, M.-X. Yang, H. Kurihara, Y.-L. Li, H. Chen, Antioxidant Xanthenes from *Swertia mussotii*, a High Altitude Plant, *Fitoterapia* 91 (2013)140-147.
- [9] C.-T. Luo, H.-H. Huang, S.-S. Mao, M.-X. Yang, C. Luo, H. Chen, Xanthenes from *Swertia mussotii* and their α -glycosidase inhibitory activities, *Planta Medica* 80 (2014) 201-208.
- [10] J. Liu, J.-R. Zhang, H.-L. Wang, Z.-J. Liu, C. Zhang, Z.-L. Jiang, H. Chen, Synthesis of xanthone derivatives and the studies on the inhibition against cancer cells growth and synergistic effects of them, *Eur. J. Med. Chem.* 133 (2017) 50-61.
- [11] Shagufta, I. Ahmad, Recent insight into the biological activities of synthetic xanthone derivatives, *Eur. J. Med. Chem.* 116 (2016) 267-280.
- [12] R. Murata, M. Horsman, Tumour-specific enhancement of thermo-radiotherapy at mild temperatures by the vascular targeting agent 5, 6-dimethylxanthenone-4-acetic acid, *Int.J. of hyperthermia*, 20 (2004) 393-404.
- [13] M. Leão, C. Pereira, A. Bisio, Y. Ciribilli, A. M. Paiva, M. Machado, A.

- Palmeira, M. X. Fernandes, E. Sousa, M. Pinto, A. Inga, L. Saraiva, Discovery of a new small-molecule inhibitor of p53/MDM2 interaction using a yeast-based approach, *Biochem. Pharm.* 85 (2013) 1234-1245.
- [14] F. Rehman, G. Rustin, Exp. ASA404: update on drug development, *Opin. Inv. Drugs* 17 (2008) 1547-1551.
- [15] J. Li, M. B. Jameson, B. C. Baguley, R. Pili, S. D. Baker, Population pharmacokinetic-pharmacodynamic model of the vascular-disrupting agent 5, 6-dimethylxanthenone-4-acetic acid in cancer patients, *Clin. Cancer Res.* 14 (2008) 2102-2110.
- [16] S. F. Zhou, P. Kestell, B. C. Baguley, J. W. Paxton, 5,6-Dimethylxanthenone -4-acetic acid (DMXAA): a new biological response modifier for cancer therapy, *Invest. New Drugs* 20 (2002) 281-295.
- [17] S. Yang, W. A. Denny, A short synthesis of 5,6-dimethylxanthenone-4-acetic acid (ASA404, DMXAA), *Tetrahedron Letters* 50 (2009) 3945-3947.
- [18] H. B. El-Serag, Hepatocellular carcinoma, *N. Engl. J. Med.* 365 (2011) 1118e1127.
- [19] S. J. Martin, C. P. M. Reutelingsperger, A. J. McGahon, J. A. Rader, R. C. A. A. van Schie, D. M. LaFace, D. R. Green, 1995. Early redistribution of plasma membrane phosphatidylserine is a general feature of apoptosis regardless of the initiating stimulus: inhibition by overexpression of Bcl-2 and Abl., *J. Exp. Med.* 182 (1995) 1545-1556.
- [20] A.G. Porter, R.U. Jänicke, Emerging roles of caspase-3 in apoptosis, *Cell. Death Differ.* 6 (1999) 99-104.
- [21] B. Shawn, S. Guy, Regulation of the Apaf-1-caspase-9 apoptosome, *J. of Cell Sci.* 123 (2010) 3209-3214.
- [22] S. W. Yu, S. A. Andrabi, H. Wang, N. S. Kim, G. G. Poirier, T. M. Dawson, V. L. Dawson, Apoptosis-inducing factor mediates poly(ADP-ribose) (PAR) polymer- induced cell death". *Proc. Natl. Acad. Sci. U.S.A.* 103 (2006) 18314-18319.
- [23] M. Leão, C. Pereira, A. Bisio, Y. Ciribilli, A. M. Paiva, N. Machado, A. Palmeira, M. X. Fernandes, E. Sousa, M. Pinto, A. Inga, L. Saraiva, Discovery of a new small- molecule inhibitor of p53-MDM2 interaction using a yeast-based approach, *Biochemical Pharmacology* 85 (2013) 1234-1245.
- [24] Lauria, M. Tutone, M. Ippolito, L. Pantano, A. M. Almerico, Molecular modeling approaches in the discovery of new drugs for anti-cancer therapy: the investigation of p53-MDM2 interaction and its inhibition by small molecules, *Curr. Med. Chem.* 17 (2010) 3142-3154.
- [25] W. Wang, Y. Hu, Small molecule agents targeting the p53-MDM2 pathway for cancer therapy, *Med. Res. Rev.* 32 (2012) 1159-1196.
- [26] Lemos, M. Leão, J. Soares, A. Palmeira, M. Pinto, L. Saraiva, M.E. Sousa, Medicinal Chemistry Strategies to Disrupt the p53-MDM2/MDMX Interaction, *Med. Res. Rev.* 36 (2016) 789-844.
- [27] P. Furet, K. Masuya, J. Kallen, T. Stachyra-Valat, S. Ruetz, V. Guagnano, P. Holzer, R. Mah, S. Stutz, A. Vaupel, Discovery of a novel class of highly

- potent inhibitors of the p53–MDM2 interaction by structure-based design starting from a conformational argument, *Bioorg. Med. Chem. Lett.* 26 (2016) 4837-4841.
- [28] Y. Rew, D. Sun, F. Gonzalez-Lopez De Turiso, M.D. Bartberger, H.P. Beck, J. Canon, A. Chen, D. Chow, J. Deignan, B. M. Fox, Structure-based design of novel inhibitors of the MDM2–p53 interaction, *J. Med. Chem.* 55 (2012) 4936-4954.
- [29] M. T. Crow, K. Mani, Y. J. Nam, R. N. Kitsis, The mitochondrial death pathway and cardiac myocyte apoptosis, *Circulation Res.*, 95 (2004) 957-970.
- [30] F. Rannou, T. S. Lee, R. H. Zhou, J. Chin, J. C. Lotz, M. A. Mayoux-Benhamou, J. P. Barbet, A. Chevrot, J. Y. J. Shyy, Intervertebral disc degeneration - The role of the mitochondrial pathway in annulus fibrosus cell apoptosis induced by overload, *Am. J. Pathology*, 164 (2004) 915-924.
- [31] Y. Otake, S. Soundararajan, T. K. Sengupta, E. A. Kio, J. C. Smith, M. Pineda-Roman, R. K. Stuart, E. K. Spicer, D. J. Fernandes, Over expression of nucleolin in chronic lymphocytic leukemia cells induces stabilization of bcl2 mRNA, *Blood*, 109 (2007) 3069–3075.
- [32] D. L. Vaux, S. Cory, J. M. Adams, Bcl-2 gene promotes haemopoietic cell survival and cooperates with c-myc to immortalize pre-B cells, *Nature*, 335 (1998) 440–442.
- [33] B. H. Mavromatis, B. D. Cheson, Novel therapies for chronic lymphocytic leukemia, *Blood Reviews*, 18 (2004) 137–148.
- [34] L. Gandhi, D. R. Camidge, M. Ribeiro de Oliveira, P. Bonomi, D. Gandara, D. Khaira, C. L. Hann, E. M. McKeegan, E. Litvinovich, Phase I study of Navitoclax (ABT-263), a novel Bcl-2 family inhibitor, in patients with small-cell lung cancer and other solid tumors, *J. Clin. Oncol.*, 29 (2011) 909–916.
- [35] R. Pan, L. J. Hogdal, J. M. Benito, D. Bucci, L. Han, G. Borthakur, J. Cortes, D. J. DeAngelo, L. Debose, Selective BCL-2 inhibition by ABT-199 causes on-target cell death in acute myeloid leukemia, *Cancer Discovery*, 4 (2014) 362–375.

1. **D-P-4** hybrid increased the activity against the growth of HepG-2 cancer cells by 460 times compared to DMXAA.
2. **D-P-4** regulated p53/MDM2 to a better healthy state than both monomers and the combination.
3. **D-P-4** showed better activity in regulating Bax/Bcl-2 to increase HepG-2 cell apoptosis.
4. **D-P-4** arrested more cells on S phase compared with any one of the two monomers or the combination.